Available online at www.sciencedirect.com

SCIENCE DIRECT®

International Journal of Mass Spectrometry 240 (2005) 149–159

International Journal of Mass Spectrometry

www.elsevier.com/locate/ijms

The aluminum phosphides Al_mP_n ($m+n=2$–5) and their anions: structures, electron affinities and vibrational frequencies

Ling Guo[a,b,*], Hai-shun Wu[a,*], Zhi-hao Jin[b]

[a] School of Chemistry and Material Science, Shanxi Normal University, Linfen 041004, China
[b] School of Material Science and Engineering, Xi'an Jiaotong University, Xi'an 710049, People's Republic of China

Received 9 September 2004; accepted 21 October 2004
Available online 26 November 2004

Abstract

Geometries, electronic states and electron affinities of Al_nP_m and $Al_nP_m^-$ ($n+m=2$–5) clusters have been examined using four hybrid and pure density functional theory (DFT) methods. Structural optimization and frequency analyses are performed with the basis of 6-311 + G (2df) one-particle basis set. The geometries are fully optimized with each DFT method independently. Three types of energy separations reported in this work are the adiabatic electron affinity (EA_{ad}), the vertical electron affinity (EA_{vert}), and the vertical detachment energy (VDE). The calculation results show that the singlet structures have higher symmetry than that of doublet structures. The best method for predicting molecular structures was found to be BLYP, while other methods generally underestimated bond lengths. The most reliable adiabatic electron affinities and vertical detachment energy, obtained at the 6-311 + G (2df)/BP86 level of theory, are 2.44 and 2.48 eV (Al_2P), 2.03 and 2.24 eV (AlP_2), 1.97 and 2.44 eV (AlP_3), 2.01 and 2.10 eV (Al_3P), 1.94 and 2.52 eV (Al_2P_2), 2.63 and 3.34 eV (AlP_4), 2.10 and 2.48 eV (Al_4P), 2.49 and 2.69 eV (Al_2P_3), 2.76 and 3.06 eV (Al_3P_2), respectively. Those for Al_2P, AlP_2, AlP_3, Al_3P, Al_4P, and Al_2P_3 are in good agreement with experiment, but the predicted VDE values for Al_2P_2, Al_3P_2, and AlP_4 are larger than the available experimental values. For the vibrational frequencies of the Al_mP_n series, the B3LYP method produces good predictions with the average error only about 10 cm^{-1} from available experimental and theoretical values. The other three methods overestimate or underestimate the vibrational frequencies, with the worst predictions given by the BLYP method.

Keywords: Density functional theory; Vibrational frequencies; Vertical electron affinity; Adiabatic electron affinity; Vertical detachment energy

1. Introduction

The chemistry and physics of the compounds formed by the elements in groups III and V is extraordinarily rich and their usefulness in the semiconductor industries has been a motivation for the numerous experimental and theoretical studies [1–6]. Among them, the aluminum phosphides have received considerable attention, as they have higher vibrational frequencies (due to lower masses), and, thus, as noted by Gomez et al. [7], could result in vibrational progressions in the spectra compared to heavier clusters. In addition, the smaller number of electrons makes them more amenable to electronic structure calculations. There have been some previous theoretical studies on Al_mP_n cluster. Costales et al. [8] have theoretically investigated the structure, stability, and vibrational properties of the $(AlP)_n$ ($n=1$–3) using both Gradient-corrected (GGA) Becke exchange functional [9] and Wang and Perdew [10] correlation functional. Archibong et al. [11,12] have reported the equilibrium geometries, harmonic vibrational frequencies and electron detachment energies of the neutral and anion AlP_2, Al_2P_2, Al_3P, and AlP_3 performed at density functional theory (DFT) (B3LYP, BP86, and BPW91-DFT) and ab inition methods [MP2 and CCSD (T)]. Feng and Balasubramanian [13–15] have also studied the structures and potential energy curves of a number of electronic states of Al_3P, AlP_3 and its positive ions, Al_2P_3, Al_3P_2 and their ions using the complete active space

---

[*] Corresponding authors. Tel.: +86 357 205 1375; fax: +86 357 205 1375.
E-mail address: gl-guoling@163.com (L. Guo).

1387-3806/$ – see front matter © 2004 Elsevier B.V. All rights reserved.
doi:10.1016/j.ijms.2004.10.018

self-consistent field (CASSCF) method followed by multireference singles and doubles configuration interaction (MRSDCI), and found the C_{3v} structure to be the global minima of AlP_3, which is different from Archibong et al. [12] prediction. Other theoretical studies on Al_mP_n and $Al_mP_n^-$ have been also published [16–20]. Gomez et al. [7] reported the experimental adiabatic electron affinity (EA_{ad}) and vertical detachment energy of Al_mP_n. The theoretical prediction of Al_mP_n electron detachment energy and electron affinities is found in the 2000–2002 study of Archibong and co workers [11,12,20] and Balasubramaniam and Feng et al. [15]. To our knowledge, this is the first time to study the geometries and electronic affinities of Al_4P and AlP_4 using density functional theory.

Density functional theory (DFT) [21,22] has evolved into a widely applicable computational technique, while requiring less computation effort than convergent quantum mechanical methods such as coupled cluster theory. The application of gradient-corrected density functionals theory has been shown to be effective for many species in groups III and V such as the Ga_xP_y, Ga_xAs_y, Al_xN_y, and In_xN_y systems [23–25]. The theoretical prediction of electron affinities has historically been generally difficult. The main reasons are the significance of electron correlation and the special requirements of the anionic systems with regard to the one-electron basis sets. Hence, in the traditional ab initio systems one needs highly correlated methods and large and flexible (in particular in the outer area which requires additional diffuse functions) basis sets. While for DFT employing local functionals there are principal difficulties with anions, from a pragmatic point of view these deficiencies are not severe; and recent work [11,12] has shown that the DFT methods are dependable for EA predictions.

The objective of the present study is to systematically apply several contemporary forms of density functional theory [21] to the determination of the electron affinities and other properties of the Al_mP_n ($m+n=2$–6) series. Of specific interest is (a) the comparison of the electron affinities with the limited available experimental results; (b) the relationship between the neutral Al_mP_n molecules and their anions as measured by the three types of energy separations, e.g., the adiabatic electron affinity (EA_{ad}), the vertical electron affinity (EA_{vert}), and the vertical detachment energy of the anion (VDE); (c) the predictions of the properties of vibrational frequencies; (d) the comparison of the different DFT methods. We would like to establish reliable theoretical predictions for those aluminum phosphides in the absence of experimental results and in some cases to challenge existing experiments.

2. Theoretical methods

The four different density functional or hybrid Hartree–Fock/density functional forms used here were as follows:

(a) Becke's 1988 exchange functional [9] with Lee et al.'s correlation functional [26] (BLYP);
(b) the half and half exchange functional [27] with the LYP correlation functional (BHLYP);
(c) Becke's three-parameter hybrid exchange functional [28a] with the LYP correlation functional (B3LYP) [28b];
(d) Becke's 1988 exchange functional with Perdew's correlation functional [29] (BP86).

Restricted methods were used for all closed-shell systems, while unrestricted methods were employed for the open-shell species. All the electron affinities and molecular structures have been determined using the Gaussian 98 [30] program suites.

The basis set followed in this study was the 6-311 + G (2df) one-particle basis set [36,37], which was similar to that employed by Archibong and St-Amant in their previous work on small clusters of germanium [31], aluminum oxides [32–34] and GaP^-/GaP_2^- [35]. Note that this basis set consists of McLean and Chandler (12s9p)/(6s5p) basis sets [36] for Al and P, augmented with two sets of five-membered d functions [$\zeta(Al)=0.65, 0.1625$; $\zeta(P)=1.1, 0.275$], a set of seven-membered f functions [$\zeta(Al)=0.25$; $\zeta(P)=0.45$] and a set of diffuse sp functions [$\zeta(Al)=0.0318$; $\zeta(P)=0.0348$].

All Al_mP_n ($m+n=2$–6) stationary point geometries were interrogated by the evaluation of their harmonic vibrational frequencies at the four different levels of theory. Zero-point vibrational energies (ZPVE) evaluated at the four levels were presented in Table 3. The ZPVE differences between Al_mP_n and $Al_mP_n^-$ ($m+n=2$–6) were quit small. These differences could be used as a correction to the adiabatic electron affinities.

The electron affinities are evaluated as the difference of total energies in the following manner:

- the adiabatic electron affinity is determined as
$$EA_{ad} = E(\text{optimized neutral}) - E(\text{optimized anion})$$
- the vertical electron affinity by
$$EA_{vert} = E(\text{optimized neutral}) - E(\text{anion at optimized neutral geometry})$$
- and the vertical detachment energy of the anion by
$$VDE = E(\text{neutral at optimized anion geometry}) - E(\text{optimized anion}).$$

3. Results and discussion

The ground state structures of Al_nP_m and $Al_nP_m^-$ ($n+m=2$–5) optimized by four hybrid and pure density functional theory (DFT) methods are shown in Fig. 1. The corresponding geometric parameters of Al_nP_m and $Al_nP_m^-$ are listed in Tables 1 and 2, respectively.

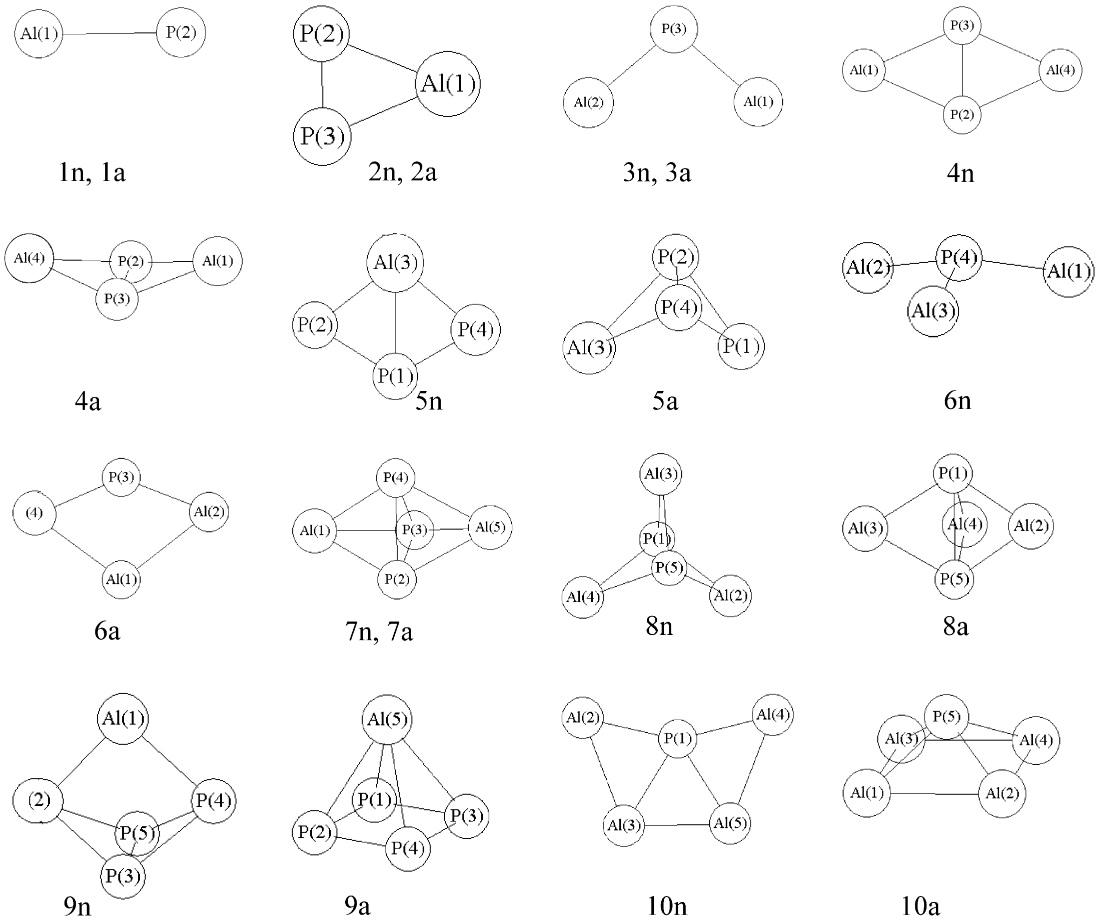

Fig. 1. Geometric configurations of the Al_mP_n and $Al_mP_n^-$ ($m+n=2$–5) clusters.

3.1. $m+n=2$

3.1.1. AlP and AlP^-

The geometries of the ground state of AlP and its anion are given in Fig. 1(1n and 1a). The neutral AlP has a X $^3\Sigma^-$ ground state and an experimental bond length of 2.40 Å [17b]. Costales et al. [8] reported a theoretical bond length of 2.460 Å at the GGA level of theory in conjunction with a double numerical basis set supplemented with d polarization functions. Theoretical bond length of 2.430 Å for AlP was also given by AL-Laham et al. [16] with the HF methods, using the 6-31G* basis set. The source of the discrepancy between the calculated and experimental bond lengths is unclear. One possible source of error lies in the fact that the experimentally determined value was spectroscopic and that the identity of the ground state is in question. Alternatively, the computational results may have some systematic error. However, the present 6-311 + G (2df) BLYP bond length (2.242 Å) provides the most favorable comparison with experiment and previous theory, while the other DFT methods predict shorter bond lengths by up to 0.028 Å (BHLYP). The general trend for bond lengths for the aluminum phosphide is BLYP > BP86 > B3LYP > BHLYP.

For the $^2\Sigma^+$ground state [17a] of the diatomic anion AlP^-, the predicted bond agree with each other to 0.032 Å among the different DFT methods, with the r_e values being roughly 0.1 Å shorter than those of the neutral species. The 6-311 + G (2df) BLYP bond length, deemed to be the most reliable, is 2.162 Å.

Our theoretical neutral–anion energy separations for AlP are given in Table 4. No experimental or other theoretical data available. The adiabatic electron affinity EA_{ad} is predicted to be 1.78 eV (BHLYP), 2.03 eV (B3LYP), 2.22 eV (BP86), and 1.95 eV (BLYP). Among them, B3LYP method is similar to the experimental result of 2.043 ± 0.020 eV. The zero-point vibrational energy correction is very small, around +0.01 eV (Table 3). The range for the theoretical vertical electron affinity EA_{vert} is 1.73–2.19 eV, and the range of VDE (AlP^-) is 1.82–2.26 eV. The general trend for EA_{ad}, EA_{vert}, and VDE for aluminum phosphides is BP86 > B3LYP > BLYP > BHLYP. The values of them are close to each other due to the small difference in geometry between the neutral and its anion.

Table 1
Geometric parameters and symmetry of neutral Al_mP_n ($m+n=2$–5)

Structure	State	Symmetry	Type L/Å (Å^{-1})	BHLYP	B3LYP	BP86	BLYP
1(n)	$^3\Sigma^-$	$C_{\infty v}$	1-2	2.214	2.224	2.226	2.242
2(n)	$^2B_2$	C_{2v}	1-2	2.579	2.609	2.610	2.643
			2-3	1.951	1.973	1.988	1.995
			2-1-3	44.4	44.4	44.8	44.9
3(n)	$^2B_2$	C_{2v}	1-3	2.230	2.238	2.241	2.253
			1-3-2	91.2	94.2	92.7	99.8
4(n)	^1A_g	D_{2h}	1-2	2.507	2.529	2.532	2.555
			2-3	2.044	2.066	2.079	2.091
			2-1-3	48.1	48.2	48.5	48.3
5(n)	$^1A_1$	C_{2v}	1-2	2.074	2.093	2.102	2.117
			1-3	2.433	2.452	2.450	2.481
			2-3	2.267	2.295	2.309	2.325
			2-1-4	119.5	120.0	120.7	120.3
			2-3-4	104.5	104.4	104.7	104.3
6(n)	$^1A_1$	C_{3v}	1-2	2.340	2.354	2.357	2.372
			1-4-2	119.9	119.9	119.9	119.9
7(n)	$^2A_2''$	D_{3h}	1-2	2.420	2.439	2.443	2.462
			2-3	2.273	2.300	2.305	2.330
8(n)	$^2A'$	C_s	1-2	2.505	2.375	2.376	2.394
			1-3	2.280	2.374	2.375	2.395
			1-4	2.506	2.570	2.555	2.594
			1-5	2.442	2.474	2.484	2.511
9(n)	$^2A_1$	C_{2v}	1-2	2.343	2.373	2.380	2.406
			2-3	2.240	2.265	2.272	2.293
			3-5	2.149	2.173	2.182	2.200
10(n)	$^2A_1$	C_{2v}	1-2	2.390	2.408	2.420	2.430
			1-3	2.445	2.462	2.464	2.487
			2-3	2.840	2.817	2.765	2.830
			3-5	2.625	2.626	2.609	2.646

3.2. $m+n=3$

3.2.1. AlP_2 and AlP_2^-

The equilibrium geometries of the $^2B_2$ ground state of neutral AlP_2 and the $^1A_1$ ground state of AlP_2^- are displayed in Fig. 1(2n and 2a). For the C_{2v} AlP_2 structure, the theoretical Al–P and P–P bond lengths are in the ranges of 2.579–2.643 Å and 1.951–1.995 Å, respectively. As was case for AlP, the BLYP method gives the longest and most reliable bond length. P–Al–P bond angles of 44.3–44.9° are predicted by four different functions. No experimental geometries are available for either AlP_2 or AlP_2^-. Feng and Balasubramanian [14] reported a theoretical bond lengths of 2.599 and 1.989 Å for Al–P and P–P bonds and a bond angle of 45.0° at the MRSDCI + Q level of theory with relativistic effective core potentials (RECPS) and 3s3p valence basis sets. Archibong et al. [11] have optimized the geometry with $r_{Al–P} = 2.603$ Å, $r_{P–P} = 1.985$ Å, $\theta = 44.8°$ at the BPw91 level, and $r_{Al–P} = 2.580$ Å, $R_{P–P} = 1.990$ Å, $\theta = 45.4°$ at the CCSD (T) level with the same basis as ours. Our BLYP results are the closest to the earlier MRSDCI + Q and CCSD (T) results. The other three DFT methods predict shorter bond distances and smaller bond angles.

The anion AlP_2^- also has C_{2v} symmetry, with the Al–P and P–P bond distances predicted to be 2.404–2.461 Å and 2.038–2.085 Å, respectively. The Al–P bond distances are about 0.2 Å shorter than their neutral counterparts, while the P–P bond distances are about 0.09 Å longer and the bond angles are about 5° larger.

The theoretical EA_{ad}, EA_{vert}, and VDE, as well as the experimental electron affinity data, are listed in Table 4. The range of EA_{ad} is from 1.72 to 2.03 eV from the four different functionals. The B3LYP result is the closest to the experiment (1.933 ± 0.007 eV) given by Gomez et al. [7] in the 2001 from their anion photoelectron spectroscopy study. BHLYP and BLYP method are smaller and BP86 method are larger than the experimental result. The range of EA_{vert} is from 1.53 to 1.84 eV and the range of VDE is from 1.94 to 2.45 eV. For the VDE, the BP86 result (2.24 eV) is very close to the experiment (2.21 ± 0.05 eV) given by Gomez et al. [7]. The values for EA_{ad}, EA_{vert}, and VDE are fairly similar due to the small differences in geometry between neutral and anion.

3.2.2. Al_2P and Al_2P^-

The geometries of the $^2B_2$ ground state of Al_2P and its $^1A_1$ ground state anion are given in Fig. 1(3n and 3a). For the C_{2v} Al_2P structure, the theoretical Al–P bond lengths are in

Table 2
Geometric parameters and symmetry of anionic Al_mP_n ($m+n=2$–5)

Structure	State	Symmetry	Type L/Å (Å^{-1})	BHLYP	B3LYP	BP86	BLYP
1(a)	$^2\Sigma^+$	$C_{\infty v}$	1-2	2.130	2.143	2.150	2.162
2(a)	$^1A_1$	C_{2v}	1-2	2.404	2.432	2.442	2.461
			2-3	2.038	2.060	2.074	2.085
			2-1-3	50.2	50.1	50.2	50.1
3(a)	$^1A_1$	C_{2v}	1-2	2.235	2.253	2.263	2.274
			2-1-3	104.0	107.3	108.0	111.8
4(a)	$^2B_1$	C_{2v}	1-2	2.413	2.434	2.440	2.460
			2-3	2.200	2.223	2.228	2.250
			2-1-3	54.2	54.3	54.3	54.4
5(a)	$^2A'$	C_s	1-2	2.144	2.165	2.173	2.191
			2-3	2.443	2.463	2.463	2.486
			2-4	2.287	2.321	2.332	2.357
			2-1-4	64.4	64.8	64.9	65.1
			2-3-4	55.8	56.2	56.5	56.6
6(a)	$^2B_2$	C_{2v}	1-2	2.747	2.720	2.678	2.726
			1-3	2.463	2.511	2.544	2.561
			2-3	2.318	2.337	2.349	2.358
7(a)	$^1A_1'$	D_{3h}	1-2	2.506	2.531	2.533	2.560
			2-3	2.220	2.242	2.247	2.268
8(a)	$^1A_1'$	D_{3h}	1-2	2.439	2.455	2.452	2.477
			1-5	2.344	2.372	2.385	2.404
9(a)	$^1A_1$	C_{4v}	1-2	2.141	2.168	2.180	2.197
			1-5	2.644	2.668	2.662	2.700
10(a)	$^1A_1$	C_{4v}	1-5	2.373	2.392	2.404	2.413
			1-5-2	77.0	76.5	74.3	77.1

the range from 2.230 to 2.253 Å and Al–P–Al bond angles of 91.2–99.8 are predicted by the four different functions. Feng and Balasubramanian [14] reported a theoretical bond length of 2.250 Å at the MRSDCI + Q level of theory with the RECPS + 3s3p basis set. Theoretical bond length and bond angle of 2.243 Å and 95.0°, respectively were also given by Gomez et al. [7] using DFT (B3LYP) with the aug-cc-pvtz basis set. Our BLYP results are the closet to the earlier MRSDCI+Q and B3LYP result. The other DFT methods predict shorter bond distances and smaller bond angles.

Table 3
Zero-point vibrational energies within the harmonic approximation for $Al_mP_n/Al_mP_n^-$ ($m+n=2$–5) in eV (kcal/mol in parentheses)[a]

Molecular	BHLYP	B3LYP	BP86	BLYP
AlP	0.028 (0.66)	0.028 (0.65)	0.029 (0.66)	0.027 (0.64)
AlP^-	0.034 (0.77)	0.033 (0.76)	0.032 (0.75)	0.032 (0.73)
AlP_2	0.075 (1.72)	0.070 (1.62)	0.069 (1.58)	0.066 (1.52)
AlP_2^-	0.082 (1.88)	0.077 (1.77)	0.076 (1.74)	0.072 (1.67)
Al_2P	0.047 (1.10)	0.046 (1.06)	0.049 (1.14)	0.048 (1.12)
Al_2P^-	0.065 (1.49)	0.062 (1.43)	0.060 (1.39)	0.059 (1.36)
Al_2P_2	0.112 (2.58)	0.107 (2.47)	0.107 (2.47)	0.102 (2.34)
$Al_2P_2^-$	0.109 (2.52)	0.104 (2.41)	0.105 (2.42)	0.099 (2.28)
AlP_3	0.149 (3.44)	0.142 (3.27)	0.140 (3.22)	0.134 (3.09)
AlP_3^-	0.129 (2.98)	0.124 (2.84)	0.125 (2.88)	0.118 (2.71)
Al_3P	0.081 (1.88)	0.080 (1.84)	0.079 (1.82)	0.078 (1.79)
Al_3P^-	0.092 (2.13)	0.090 (2.08)	0.093 (2.14)	0.087 (2.00)
Al_2P_3	0.183 (4.23)	0.179 (4.13)	0.181 (4.18)	0.171 (3.95)
$Al_2P_3^-$	0.180 (4.14)	0.172 (3.96)	0.174 (4.00)	0.163 (3.75)
Al_3P_2	0.146 (3.36)	0.127 (2.92)	0.134 (3.08)	0.128 (2.95)
$Al_3P_2^-$	0.149 (3.43)	0.144 (3.33)	0.146 (3.38)	0.138 (3.19)
AlP_4	0.205 (4.72)	0.191 (4.41)	0.187 (4.31)	0.134 (3.09)
AlP_4^-	0.203 (4.68)	0.190 (4.39)	0.187 (4.32)	0.178 (4.11)
Al_4P	0.115 (2.65)	0.113 (2.61)	0.116 (2.68)	0.108 (2.50)
Al_4P^-	0.124 (2.86)	0.120 (2.77)	0.125 (2.87)	0.113 (2.61)

[a] All results obtained with the 6-311 + G (2df) basis set.

With attachment of an extra electron to the neutral Al_2P to form the Al_2P^- anion, the symmetry does not change, but the Al–P–Al bond angle changes by 12–16°, and the Al–P bond lengths are longer than those of the neutral by −0.03 Å.

Our theoretical neutral–anion energy separations for Al_2P, as well as experimental data, are given in Table 4. The adiabatic electron affinity EA_{ad} predicted to be 2.35 eV (BHLYP), 2.40 eV (B3LYP), 2.44 eV (BP86), and 2.19 eV (BLYP). The theoretical values are all lower than the experimental value (2.513 ± 0.02 eV) reported by Gomez et al. [7] and the BP86 result (2.44eV) provides the most favorable comparison with experiment. The range for the theoretical vertical electron affinity EA_{vert} is from 2.16 to 2.38 eV, among which the BP86 method again predicts the largest and most reliable value (2.38 eV). The range of VDE (Al_2P^-) is 2.23–2.37 eV, and thus, the anion is quit stable with respect to electron detachment. And the BP86 method also predicts the largest and reasonable value according to the experimental value of 2.55 ± 0.025 eV. The values of EA_{ad}, EA_{vert}, and VDE are close to each other due to the small different geometry between the neutral and its anion.

Table 4
Adiabatic and vertical electron affinities of the neutral Al_mP_n ($m+n=2$–5) and vertical detachment energies of their anions in eV (kcal/mol in parentheses)[a]

Molecular	Method	EA_{ad}	EA_{vert}	VDE
AlP	BHLYP	1.78 (41.02)	1.73 (39.88)	1.82 (42.08)
	B3LYP	2.03 (46.92)	1.99 (45.91)	2.07 (47.78)
	BP86	2.22 (51.32)	2.19 (50.44)	2.26 (52.17)
	BLYP	1.95 (44.91)	1.91 (44.03)	1.98 (45.79)
	Experimental[b]	2.043 ± 0.020		
AlP_2	BHLYP	1.79 (41.33)	1.55 (35.68)	2.45 (56.66)
	B3LYP	1.91 (44.16)	1.69 (39.07)	2.14 (49.50)
	BP86	2.03 (46.92)	1.84 (42.46)	2.24 (51.69)
	BLYP	1.72 (39.76)	1.53 (35.24)	1.94 (44.78)
	Experimental[c]	1.933 ± 0.007		2.21 ± 0.025
Al_2P	BHLYP	2.35 (54.14)	2.31 (53.26)	2.37 (54.77)
	B3LYP	2.40 (55.40)	2.36 (54.58)	2.42 (55.96)
	BP86	2.44 (56.22)	2.38 (55.02)	2.48 (57.16)
	BLYP	2.19 (50.63)	2.16 (49.93)	2.23 (51.57)
	Experimental[c]	2.513 ± 0.02		2.55 ± 0.025
Al_2P_2	BHLYP	1.83 (42.27)	1.46 (33.60)	2.36 (54.46)
	B3LYP	1.88 (43.40)	1.53 (35.36)	2.38 (54.90)
	BP86	1.94 (44.78)	1.68 (38.88)	2.52 (58.10)
	BLYP	1.66 (38.38)	1.34 (30.84)	2.17 (50.06)
	Experimental[c]	2.15 ± 0.1		2.33 ± 0.025
AlP_3	BHLYP	1.95 (44.91)	1.21 (27.93)	2.39 (55.27)
	B3LYP	1.89 (43.72)	1.59 (36.62)	2.34 (54.02)
	BP86	1.97 (45.41)	1.64 (37.88)	2.44 (56.28)
	BLYP	1.62 (37.31)	1.40 (32.28)	2.05 (47.23)
	Experimental[c]	2.06 ± 0.05		2.58 ± 0.05
Al_3P	BHLYP	1.43 (33.10)	0.58 (13.38)	2.01 (46.54)
	B3LYP	1.62 (37.37)	0.75 (17.21)	2.04 (47.09)
	BP86	2.01 (46.35)	0.90 (20.72)	2.10 (48.55)
	BLYP	1.45 (33.42)	0.57 (13.13)	1.79 (41.33)
	Experimental[c]	2.051 ± 0.02		2.21 ± 0.025
Al_2P_3	BHLYP	2.45 (56.55)	2.26 (52.26)	2.64 (60.93)
	B3LYP	2.48 (57.28)	2.29 (52.82)	2.69 (62.12)
	BP86	2.49 (57.47)	2.29 (52.82)	2.69 (62.12)
	BLYP	2.26 (52.26)	2.06 (47.61)	2.48 (57.16)
	Experimental[c]	2.739 ± 0.02		2.92 ± 0.025
Al_3P_2	BHLYP	2.67 (61.68)	2.39 (55.09)	3.49 (80.59)
	B3LYP	2.73 (63.02)	2.54 (58.60)	3.06 (70.73)
	BP86	2.76 (63.82)	2.59 (59.86)	3.06 (70.73)
	BLYP	2.49 (57.47)	2.31 (53.26)	2.81 (64.76)
	Experimental[c]	2.58 ± 0.05		2.82 ± 0.025
AlP_4	BHLYP	2.41 (55.59)	1.39 (31.97)	3.23 (74.56)
	B3LYP	2.57 (59.29)	1.52 (35.05)	3.37 (77.76)
	BP86	2.63 (60.61)	1.55 (35.74)	3.34 (77.13)
	BLYP	2.42 (55.78)	1.37 (31.59)	3.26 (75.31)
	Experimental[c]	2.64 ± 0.05		2.93 ± 0.025
Al_4P	BHLYP	1.77 (40.86)	1.72 (39.63)	2.11 (48.68)
	B3LYP	1.92 (44.32)	1.82 (42.08)	2.27 (52.32)
	BP86	2.10 (48.43)	1.92 (44.32)	2.48 (57.35)
	BLYP	1.73 (39.95)	1.64 (37.81)	2.10 (48.43)
	Experimental[c]	1.98 ± 0.05		2.40 ± 0.025

[a] Values are not corrected for ZPVE and were obtained with the 6-311 + G (2df) basis set.

[b] Ref. [17a].

[c] Ref. [7].

3.3. $m+n=4$

3.3.1. Al_2P_2 and $Al_2P_2^-$

The equilibrium structures of the ^1A_g ground state of neutral Al_2P_2 and the $^2B_1$ ground of $Al_2P_2^-$ are displayed in Fig. 1(4n and 4a). For the D_{2h} Al_2P_2 structure, the theoretical Al–P and P–P bond lengths are in the ranges of 2.507–2.555 Å and 2.044–2.091 Å, respectively, and P–Al–P bond angles of 48.4–48.5° are predicted by the four different functions. Costales et al. [8] reported a theoretical Al–P and P–P bond lengths of 2.530 and 2.080 Å and a bond angle of 48° at the GGA/DNP level of theory. Al-Laham et al. [16] using HF/6-31G(d) theory reported 2.530, 2.040 Å and 48°, their work seems to underestimate the P–P distance due to neglect of electron correlation. Our BLYP results are the closest to the earlier GGA/DNP and HF results. The other three DFT methods predict shorter bond distances.

The anionic $Al_2P_2^-$ is found to have a no planar C_{2v} distorted tetrahedron ground state ('butterfly' structure), which is different from Feng's [19] prediction of D_{2h} geometry, and in agreement with the results of Archibong [11] and Gomez [7]. Adding an electron makes the Al–P bond distances are about 0.1 Å shorter than their neutral counterparts, while the P–P bond distances are about 0.2 Å longer.

The theoretical EA_{ad}, EA_{vert}, and VDE, as well as the experimental EA_{ad} and VDE data, are listed in Table 4. The range of EA_{ad} is from 1.66 to 1.94 eV from the four different functionals, and these values are all smaller than the experimental values (2.15 ± 0.1 eV). The BP86 method predicts the largest EA_{ad} for Al_2P_2 (1.94 eV), and it should be recognized as the most reliable value based on the experimental result. The range of EA_{vert} is from 1.34 to 1.68 eV and the range of VDE is from 2.17 to 2.52 eV. The BHLYP result for VDE (2.36 eV) is the closest to the experiment (2.33 ± 0.025 eV). The other three DFT methods predict smaller or larger value. Again, the differences between EA_{ad}, EA_{vert}, and VDE are due to the change in the geometry between Al_2P_2 and $Al_2P_2^-$.

3.3.2. AlP_3 and AlP_3^-

The geometries of the ground state of AlP_3 and its anion are displayed in Fig. 1(5n and 5a). The neutral AlP_3 molecule, like the valence isoelectronic $AlAs_3$, has C_{2v} symmetry for the $^1A_1$ ground state. AlP_3 is a stable clusters, and many experimental and theoretical studies have been reported. Liu et al. [38] have observed the AlP_3^- cluster in TOF. Gomez et al. [7] reported the experimental adiabatic electron affinity (2.06 ± 0.05 eV) and vertical detachment energy (2.58 ± 0.05 eV) for AlP_3. The previous theoretical studies of the AlP_3 geometry include the 1999 work by Feng and Balasubramanian [13] at the ab initio CASSCF/MRSDCI level of theory with the RECPs + 3s3p basis sets, and the 2002 work by Archibong et al. [12] with the B3LYP-DFT, MP2, and CCSD (T) methods. Feng's studies appeared to have established the ground state geometry of AlP_3 to be the pyramidal C_{3v} ($^3A_2$) structure. They reported the Al–P and P–P bond distances and the P–Al–P bond angle to be 2.780, 2.165 Å and 45.8°, respectively. While Archibong et al. gave the different conclusion. They found two singlet states ($^1A_1$-C_{2v} and $^1A'$-C_s) were nearly degenerate and lower in energy by at least 0.5 eV than the triplet ($^3A_2$-C_{3v}) state previously predicted by Feng et al. as the ground electronic state of AlP_3, and predicted the C_{2v} structure to be the ground state of AlP_3. They reported the two Al–P, P–P bond distances and P–Al–P, P–P–P bond angles to be 2.297, 2.454, 2.092 Å and 104.2°, 120.1°; 2.332, 2.442 and 2.072 Å and 102.8°, 123.1°, at the B3LYP and MP2 levels of theory, respectively. Our optimized AlP_3 ground state is consistent with Archibong's result, and our BLYP results are close to Archibong's results. Other three DFT functionals predict shorter bonds. The bond angles from the different theoretical methods change only slightly.

The $^2A'$ ground state of the AlP_3^- anion is predicted to have a three-dimensional distorted tetrahedron structure with C_s-symmetry (Fig. 1(5a)). The trend for the theoretical bond lengths with the different theoretical methods is similar to that for the neutral cluster, i.e., BLYP > BP86 > B3LYP > BHLYP. The DFT P–Al–P and P–P–P bond angles range from 55.8° to 56.6° and from 64.4° to 65.1°, respectively. The BLYP method predicts the geometrical parameters to be $r(Al_3–P_2) = 2.486$ Å, $r(P_1–P_2) = 2.191$ Å, $r(P_2–P_4) = 2.357$ Å, and $\angle$P–Al–P = 56.6°, $\angle$P–P–P = 65.1°, which are close to Archibong's results of 2.482 Å, 2.144 Å, 2.319 Å, 55.7° and 65.5°, respectively. We also tried to optimized structures for the $C_{\infty v}$, C_{2v}, C_{3v} and other C_s symmetry reported by Archibong and St-Amant for $AlAs_3^-$ [39], but these stationary points all have higher energies and some have one imaginary vibrational frequencies.

The theoretical EA_{ad}, EA_{vert}, and VDE are listed in Table 4. The predicted EA_{ad} for AlP_3 ranges from 1.62 to 1.97 eV, which are all lower than the experimental value of 2.06 ± 0.05 eV. Among them the BP86 method predicts the largest value (1.97 eV) for AlP_3, and it should be regard as the most reliable value according to the experiment. The EA_{vert} values are ranging from 1.21 to 1.59 eV, while the VDE value are large and vary from 2.05 to 2.44 eV, which are also all lower than the experimental value of 2.58 ± 0.05 eV with the BP86 method most reasonable. One readily sees that the values for EA_{ad}, EA_{vert}, and VDE are different due to the difference in geometries between the neutral AlP_3 (distorted rhombus) and the anion AlP_3^- (distorted tetrahedron).

3.3.3. Al_3P and Al_3P^-

The C_{3v}-symmetry structure of the $^1A_1$ ground state for the neutral Al_3P and the C_{2v}-symmetry structure of the $^2B_2$ ground state for the anionic Al_3P^- are shown in Fig. 1(6n and 6a). The Al–P bond distance and Al–P–Al bond angle obtained by Feng and Balasubramanian [13] at the CASSCF level were reported as 2.368 Å and 111.7°, respectively. Our BLYP result of 2.372 Å (for Al–P bond) agrees very well with theirs results. Our other three DFT functionals predict shorter Al–P bonds with the shortest being the value 2.340 Å given by BHLYP. The bond angles from the different theoretical methods are same (119.9°) and larger than Ref. [13].

The C_{2v} symmetry of the $^2B_2$ ground state Al_3P^- is given in Fig. 1(6a). The $Al_1–P_3$ bond lengths given by the four DFT methods are shorter than those for the $Al_2–P_3$ bonds, by −0.2 Å, and the two Al–P bonds are shorter than the Al–Al bonds by the four DFT methods. Archibong et al. [20] reported the $Al_1–Al_2$, $Al_1–P_3$ and $Al_2–P_3$ bond distances as 2.750, 2.468, and 2.338 Å at the MP2/6-311 + G (2df) level, and 2.716, 2.512, and 2.343 Å at the CCSD (T) level, respectively. Our B3LYP method predicts the 2.720, 2.511, and 2.337 Å for the $Al_1–Al_2$, $Al_1–P_3$ and $Al_2–P_3$ bonds, giving the most reliable bond lengths for comparison with the MP2 and CCSD (T).

The EA_{ad}, EA_{vert}, and VDE values are reported in Table 4. Our predicted EA_{ad} is in the range from 1.43 to 2.01 eV, among which the BP86 method predicts the largest value, $EA_{ad} = 2.01$ eV, which is very closest to the experimental value of 2.051 ± 0.02 eV. The range of EA_{vert} is predicted from 0.58 to 0.90 eV. The range of VDE is from 1.79 to 2.10 eV. Again, the BP86 method yields the highest and most reasonable VDE value. The BLYP method yields the smallest EA_{ad}, but this is not the case for EA_{vert} and VDE. Archibong and St-Amant [20] also gave their calculated VDE of 1.95, 2.04, and 2.04 eV at the MP2, B3LYP and CCSD (T) levels, respectively, agree also very well with experimental and our calculations.

3.4. $m + n = 5$

3.4.1. Al_2P_3 and $Al_2P_3^-$

Both Al_2P_3 and $Al_2P_3^-$ have D_{3h} trigonal bipyramidal structure, which are given in Fig. 1(7n and 7a). For the neutral $^2A_1''$ ground state, the Al–P bond lengths given by the four DFT methods are all longer than those for the P–P bonds, by −0.2 Å. Balasubramanian and Feng [15] studied the Al_2P_3 structure. They reported the Al–P and P–P distance to be 2.434 and 2.300 Å, respectively, using the CASSCF/MRSDCI level of theory with the RECPs + 3s3p basis sets. Our B3LYP and BP86 bond distance 2.439 and 2.300 Å are all close to the Balasubramanian and Feng [15] prediction.

For the $^1A_1'$ ground state of $Al_2P_3^-$, the symmetry dose not change, but the P–P bond lengths are shorter than those of the neutral species by −0.06 Å, and the Al–P bond lengths are longer by −0.1 Å. Balasubramanian and Feng [15] also optimized the anionic $Al_2P_3^-$ structure, predicting the bond distances to be 2.523 Å (Al–P) and 2.263 Å (P–P) at the CASSCF level. Their bond lengths are in good agreement with our BLYP bond distances.

The theoretical EA_{ad}, EA_{vert}, and VDE, as well as the experimental EA_{ad} and VDE data, are listed in Table 4. The range of EA_{ad} is from 2.26 to 2.49 eV, and these values are all smaller than the experimental values (2.739 ± 0.02 eV). Again, the BP86 method predicted the largest EA_{ad} for Al_2P_3 (2.49 eV) and is also closest to the experiment. The range of

EA_{vert} is from 2.06 to 2.29 eV and the range of VDE is from 2.48 to 2.64 eV. The four theoretical values of VDE are all smaller than the experimental value (2.92 ± 0.025 eV), and both BP86 and B3LYP method have the highest and reasonable VDE (2.69 eV). The values for EA_{ad}, EA_{vert}, and VDE are fairly similar due to the small differences in geometry between neutral and anion, like those for AlP_2 and Al_2P discussed above.

3.4.2. Al_3P_2 and $Al_3P_2^-$

The C_s-symmetry structure of the $^2A'$ ground state for the neutral Al_3P_2 and the D_{3h}-symmetry structure of the $^1A'_1$ ground state for the anionic $Al_3P_2^-$ are shown in Fig. 1(8n and 8a). Feng and Balasubramanian [19] reported a distorted trigonal bipyramid structure with C_{2v} ($^2A_1$) symmetry as the ground state. Our optimized BHLYP result is in agreement with their conclusion, but the other three DFT methods predict this C_{2v} structure a transition state with an imaginary frequencies at 26.6, 132.9, and 140.7 $i\,cm^{-1}$, respectively. Further optimizations result in a geometry with lower C_s symmetry, which is more stable than the C_{2v} one by 0.10, 0.11, 0.79, and 1.05 kJ mol^{-1} at the BHLYP, B3LYP, BP86, and BLYP levels, respectively.

The $Al_3P_2^-$ ion displays D_{3h} symmetry, which is in agreement with Feng and Balasubramanian [19] prediction. The BLYP method predicts the longest Al–P (2.477 Å) and P–P (2.404 Å) bond distances compared well with Feng's values of 2.474 and 2.420 Å, respectively, obtained using CASSCF level of theory with the RECPs + 3s3p basis set.

The theoretical EA_{ad}, EA_{vert}, and VDE, as well as the experimental data, are listed in Table 4. The range of EA_{ad} is from 2.49 to 2.76 eV from the four different functionals, these values are all larger than the experimental values (2.58 ± 0.05 eV) except for the BLYP value (2.49 eV). The BHLYP result (2.67 eV) is the closest to the experiment. The EA_{vert} values are ranging from 2.31 to 2.59 eV, and the VDE values are large and vary from 2.81 to 3.49 eV with BLYP value (2.81 eV) the closest to the experiment (2.82 ± 0.025 eV). One readily sees that the values for EA_{ad}, EA_{vert}, and VDE are different due to the large difference in structures between the neutral and anion.

3.4.3. AlP_4 and AlP_4^-

The C_{2v}-symmetry geometry of the $^2A_1$ ground state for AlP_4 and the square pyramidal structure of C_4-symmetry for the $^1A_1$ ground state for AlP_4^- are given in Fig. 1(9n and 9a). The neutral AlP_4 can be seen as a tetrahedral P_4 structure with a two-fold Al atom bond to it, which is similar with the valence-isoelectronic $GaAs_4$ reported by Piquini et al. [40], and this similar proves the Gomez's prediction [7] that small AlP clusters adopt the two- and three-dimensional characteristic of Ga_xAs_y clusters. There exists two kinds of P–P and one Al–P bonds in the neutral ground state, and the Al–P bond lengths given by the four DFT methods are all longer than those for P–P bonds, by about 0.1 and 0.2 Å, respectively. The BLYP method, deemed to be the most reliable, gives the bond lengths of 2.406 Å (for Al–P), 2.293 Å (for P_2–P_3) and 2.200 Å (for P_3–P_5). The other methods predict bond distances shorter by up to 0.1 Å. We also tried to optimize structures for the C_{4v}, C_s, and other C_{2v} symmetry of $GaAs_4$, but these stationary points all have higher energies and some have one imaginary vibrational frequency.

With attachment of an extra electron to the neutral AlP_4 to form the AlP_4^- anion, the symmetry changes from C_{2v} to C_{4v}, the Al–P bond distances are longer than those of the neutral species by about 0.3 Å. And the four same Al–P bond distances are still longer than its four same P–P bonds by about 0.5 Å in the four DFT methods.

The theoretical EA_{ad}, EA_{vert}, and VDE, as well as the experimental data, are listed in Table 4. Unlike GaP_4, which has a very large experimental EA_{ad} (3.45 eV) [41] value, the predicted EA_{ad} for AlP_4 ranges from 2.41 to 2.63 eV, among which the BP86 method gives the highest EA_{ad} (2.63 eV), and the value is also closest to the experimental result (2.64 ± 0.05 eV). Thus, we predict a difference between the EAs of GaP_4 and AlP_4. The EA_{vert} ranges from 1.37 to 1.55 eV. The VDE ranges from 3.23 to 3.37 eV, indicating that the anion is quit stable with respect to electron detachment. The four theoretical values of VDE are all higher than the experimental value (2.93 ± 0.025 eV), and the BHLYP method has the lowest and reasonable VDE (3.23 eV). Again, the differences between EA_{ad}, EA_{vert}, and VDE are due to the changes in geometry between AlP_4 and AlP_4^-.

3.4.4. Al_4P and Al_4P^-

The C_{2v}-symmetry structure of the $^2A_1$ ground state for the neutral Al_4P and the C_{4v}-symmetry structure of the $^1A_1$ ground state for the anionic Al_4P^- are shown in Fig. 1(10n and 10a). No other theoretical data available. For the neutral Al_4P, the P_1–Al_2 bond lengths given by the four DFT methods are shorter than those for the P_1–Al_3 bonds, by −0.06 Å, which are all shorter than the Al_2–Al_3 and Al_2–Al_5 bonds. The BLYP method gives the longest bond lengths of 2.430 Å (for P_1–Al_2), 2.487 Å (for P_1–Al_3), 2.830 Å (for Al_2–Al_3) and 2.646 Å (for Al_3–Al_5). The other methods predict bond distances shorter by up to 0.1 Å. The BLYP bond distances are considered to be the most reliable results based on the calculations above.

With attachment of an extra electron to the neutral Al_4P to form the Al_4P^- anion, the geometry changes greatly. The Al_4P^- anion displays C_{4v} symmetry, and it has shorter Al–P bond distances than the neutral. The qualitative structural differences show that bonding in the Al_4P^- anion is quit distinct from that for the neutral species.

The theoretical EA_{ad}, EA_{vert}, and VDE, as well as the experimental data, are listed in Table 4. The BP86 method gives the highest EA_{ad} (2.10 eV), EA_{vert} (1.92 eV), and VDE (2.48 eV), which are higher but the closest to the corresponding experimental values (1.98 ± 0.05 eV for EA_{ad} and 2.40 ± 0.025 eV for VDE). Our other three functionals predict lower results with the lowest being the value 1.73, 1.64, and 2.10 eV given by BLYP. Again, the differences between

Table 5
Harmonic vibrational frequencies (cm^{-1}) for Al$_m$P$_n$ ($m + n = 2$–5)

	Symmetry	BHLYP	B3LYP	BP86	BLYP	Experimental and other theory
AlP	σ	459	457	464	446	348 [8,17a] 381[14] 379 [17a]
AlP$_2$	b_2	168	155	153	139	140 [14] 157 [11]
	a_1	303	285	284	268	271 [14] 286 [11] 306 [7]
	a_1	735	692	670	654	650 [14] 693 [11]
Al$_2$P	a_1	79	68	51	67	69 [7] 76 [14]
	b_2	254	241	304	304	230 [7] 208 [14]
	a_1	445	435	441	415	421 [7] 430 [7] 435 [14]
AlP$_3$	b_1	206	196	190	187	196 [12] 191 [12]
	a_1	309	292	288	274	291 [12] 281 [12]
	b_2	373	359	359	337	358 [12] 367 [12]
	a_1	387	367	360	348	367 [12] 368 [12]
	a_1	533	504	494	474	504 [12] 521 [12]
	b_2	595	571	567	541	571 [12] 653 [12]
Al$_3$P	a_1	4	20	18	30	
	e	71	70	67	70	
	a_1	310	297	293	284	
	e	429	415	412	399	
Al$_2$P$_2$	b_{3u}	91	87	84	84	88 [11] 92 [8]
	b_{2u}	163	159	164	153	159 [11] 164 [8]
	b_{3g}	281	275	276	263	274 [11] 277 [8]
	a_g	285	277	288	265	276 [11] 289 [8]
	b_{1u}	357	341	339	323	340 [11] 341 [8]
	a_g	625	598	575	555	588 [11] 572 [8]
Al$_2$P$_3$	e'	183	177	178	169	175 [15]
	a''_2	268	304	342	324	309 [15]
	e''	312	317	313	291	303 [15]
	a'_1	358	343	342	327	339 [15]
	e'	408	386	384	364	379 [15]
	a'_1	522	492	488	463	482 [15]
Al$_3$P$_2$	a'	96	45	91	96	
	a'	117	115	121	121	
	a'	190	122	152	162	
	a''	207	169	191	164	
	a'	248	263	261	252	
	a''	270	281	288	267	
	a''	363	296	298	284	
	a'	368	328	330	311	
	a'	489	425	423	405	
AlP$_4$	a_1	258	243	232	231	
	a_1	364	338	335	316	
	b_2	403	375	370	348	
	a_1	438	409	402	381	
	b_2	471	437	427	404	
	a_1	579	544	534	512	
Al$_4$P	b_1	36	31	9	24	
	a_2	74	70	62	65	
	a_1	100	107	124	104	
	b_2	114	132	156	130	
	b_2	189	182	193	172	
	a_1	279	271	274	261	
	a_1	285	284	300	272	
	a_1	364	354	358	339	
	b_2	411	397	394	380	

EA_{ad}, EA_{vert}, and VDE are due to the changes in geometry between Al_4P and Al_4P^-.

4. Vibrational frequencies

Harmonic vibrational frequencies have been predicted for each neutral molecule with each functional, and these are reported in Table 5. Available experimental fundamentals [7] and other theoretical prediction [8,11,12,14,15,17] are included for comparison. The B3LYP method gives the best predictions for the harmonic vibrational frequencies of the Al_mP_n series, compared to the limited experimental values and other theoretical results in Table 5. For the Al_mP_n molecules, the average error for the B3LYP method is only about 10 cm^{-1}. The other three methods underesti-

Table 6
Harmonic vibrational frequencies (cm^{-1}) for anionic $Al_mP_n^-$ ($m + n = 2–5$)

	Symmetry	BHLYP	B3LYP	BP86	BLYP	Experimental and other theory
AlP^-	σ	542	529	525	509	551 [17a]
AlP_2^-	b_2	305	290	290	274	286 [7] 304 [11]
	a_1	384	360	354	339	358 [7] 378 [11]
	a_1	627	590	574	554	585 [7] 578 [11]
Al_2P^-	a_1	88	79	75	73	78 [7]
	a_1	454	429	419	402	426 [7] 450 [7]
	b_2	503	489	481	475	498 [7]
AlP_3^-	a'	154	157	173	154	157 [12] 182 [12]
	a''	211	215	236	215	215 [12] 29 [12]
	a'	325	307	305	289	307 [12] 322 [12]
	a'	405	378	370	353	378 [12] 389 [12]
	a''	407	391	395	373	391 [12] 405 [12]
	a'	577	545	536	511	545 [12] 518 [12]
Al_3P^-	b_1	67	68	68	68	68 [20] 97 [20]
	a_1	135	145	173	147	144 [20] 127 [20]
	b_2	231	222	219	208	243 [20] 245 [20]
	a_1	240	244	270	240	222 [20] 247 [20]
	a_1	385	369	366	351	369 [20] 381 [20]
	b_2	429	408	399	389	409 [20] 438 [20]
$Al_2P_2^-$	a_1	68	71	79	73	
	b_1	199	196	203	188	
	a_2	257	245	252	228	
	a_1	323	307	304	290	
	b_2	420	398	391	375	
	a_1	494	468	464	442	
$Al_3P_2^-$	e'	113	113	114	112	116 [15]
	e''	215	216	235	209	217 [15]
	a_2''	249	241	245	231	241 [15]
	a_1'	287	272	268	259	268 [15]
	e'	386	370	369	351	368 [15]
	a_1'	438	417	415	397	411 [15]
$Al_2P_3^-$	e'	153	147	151	140	146 [15]
	e''	246	241	256	230	245 [15]
	a_1'	320	305	305	289	304 [15]
	a_2''	388	368	365	347	367 [15]
	e'	423	402	402	380	394 [15]
	a_1'	545	517	513	488	504 [15]
AlP_4^-	e	168	163	175	154	
	a_1	318	304	307	288	
	e	489	455	444	423	
	a_1	539	500	486	466	
Al_4P^-	e	85	90	117	79	
	a_1	110	106	123	95	
	b_2	109	107	110	104	
	b_1	172	160	172	142	
	b_2	238	228	225	220	
	a_1	371	357	363	339	
	e	415	399	390	383	

mate or overestimate the harmonic vibrational frequencies in the Al_mP_n series, with the worst predictions given by BLYP method. Note that this emphasizes the necessity of being very selective in choosing DFT results for the theory predictions. While the BLYP method is excellent for the structures of this $Al_mP_n/Al_mP_n^-$ system, the vibrational frequencies predicted by this method is generally unreliable. The harmonic vibrational frequencies for the anionic $Al_mP_n^-$ systems are listed in Table 6, which were also reported by Gomez [7], Archibong et al. [11,12,20], and Balasubramanian and Feng [15]. Our B3LYP vibrational frequencies for $Al_mP_n^-$ are in good agreement with their results.

5. Conclusions

Carefully selected DFT methods applied with the 6-311 + G (2df) basis set are capable of reliable predicting the available experimental structures, EAs, and vibrational frequencies for the neutral and anionic aluminum phosphides clusters. The BLYP method is the most reliable method for predicting the geometries, and BP86 method is reliable for electron affinities and vertical detachment energy of these systems. The adiabatic electron affinities and vertical detachment energy are predicted to be 2.44 and 2.48 eV (Al_2P), 2.03 and 2.24 eV (AlP_2), 1.97 and 2.44 eV (AlP_3), 2.01 and 2.10 eV (Al_3P), 1.94 and 2.52 eV (Al_2P_2), 2.63 and 3.34 eV (AlP_4), 2.10 and 2.48 eV (Al_4P), 2.49 and 2.69 eV (Al_2P_3), 2.79 and 3.06 eV (Al_3P_2), respectively. Those for Al_2P, AlP_2, AlP_3, Al_3P, Al_4P, Al_2P_3, and Al_3P_2 are in good agreement with experiment, but the predicted VDE values for Al_2P_2, Al_3P_2, and AlP_4 are larger than the available experimental values. For the vibrational frequencies of the Al_mP_n series, the B3LYP method produces good predictions with the average error only about 10 cm^{-1} from available experimental and theoretical values. The other three methods overestimate or underestimate the vibrational frequencies, with the worst predictions given by the BLYP method.

References

[1] C.C. Anrnold, D.M. Neumark, J. Chem. Phys. 99 (1994) 3353.
[2] G.R. Burton, C. Xu, C.C. Arnold, D.M. Neumark, J. Chem. Phys. 104 (1996) 2757.
[3] K.R. Asmis, T.R. Taylor, D.M. Neumark, J. Chem. Phys. 111 (1999) 8838.
[4] K.R. Asmis, T.R. Taylor, D.M. Neumark, J. Chem. Phys. 111 (1999) 10491.
[5] T.R. Taylor, K.R. Asmis, C.S. Xu, D.M. Neumark, Chem. Phys. Lett. 297 (1998) 133.
[6] S. Li, R.J. Van Zee, W. Weltner Jr., J. Phys. Chem. 97 (1993) 11393.
[7] H. Gomez, T.R. Taylor, D.D. Neumark, J. Phys. Chem. A 105 (2001) 6886.
[8] A. Costales, A.K. Kandalam, R. Franco, R. Pandey, J. Phys. Chem. B 106 (2002) 1940.
[9] A.D. Becke, Phys. Rev. A 38 (1988) 3098.
[10] Y. Wang, J.P. Perdew, Phys. Rev. A 43 (1991) 8911.
[11] E.F. Archibong, R.M. Gregorius, S.A. Alexander, Chem. Phys. Lett. 321 (2000) 253.
[12] E.F. Archibong, S.K. Goh, D.S. Marynick, Chem. Phys. Lett. 361 (2002) 214.
[13] P.Y. Feng, K. Balasubramanian, Chem. Phys. Lett. 301 (1999) 458.
[14] P.Y. Feng, K. Balasubramanian, Chem. Phys. Lett. 318 (2000) 417.
[15] K. Balasubramanian, P.Y. Feng, J. Phys. Chem. A 105 (2001) 11295.
[16] M.A. Al-Laham, G.W. Trucks, K. Raghavachari, J. Chem. Phys. 96 (1992) 1137.
[17] (a) H. Gomez, T.R. Taylor, Y. Zhao, D.M. Neumark, J. Chem. Phys. 117 (2002) 8644;
(b) A. Tomasulo, M.V. Ramakrishna, J. Chem. Phys. 105 (1996) 10449.
[18] P.J. Bruna, F. Grein, J. Phys. B: At., Mol. Opt. Phys. 22 (1989) 1913.
[19] P.Y. Feng, K. Balasubramanian, J. Phys. Chem. A 103 (1999) 9093.
[20] E.F. Archibong, A. St-Amant, J. Phys. Chem. A 106 (2002) 5932.
[21] (a) P. Hohenberg, W. Kohn, Phys. Rev. B 136 (1964) 864;
(b) W. Kohn, L. Sham, Phys. Rev. A 140 (1965) 1133.
[22] W. Kohn, A.D. Becke, R.G. Parr, J. Phys. Chem. 100 (1996) 12974.
[23] E.F. Archibong, A. St-Amant, Chem. Phys. Lett. 316 (2000) 151.
[24] S.K. Nayak, S.N. Khanna, P. Jena, Phys. Rev. B 57 (1998) 3787.
[25] A. Costales, R. Pandey, J. Phys. Chem. A 107 (2003) 192.
[26] C. Lee, W. Yang, R.G. Parr, Phys. Rev. B 37 (1993) 785.
[27] A.D. Becke, J. Chem. Phys. 98 (1993) 1372.
[28] (a) A.D. Becke, J. Chem. Phys. 98 (1993) 5648;
(b) Stephens, J. Phys. Chem. 98 (1994) 11623.
[29] J.P. Perdew, Phys. Rev. B 34 (1986) 7406.
[30] M.J. Frisch, G.W. Trucks, H.B. Schlegel, G.E. Scuseria, M.A. Robb, J.R. Cheeseman, V.G. Zakrzewski, J.A. Montgomery Jr., R.E. Stratmann, J.C. Burant, S. Dapprich, J.M. Millam, A.D. Daniels, K.N. Kudin, M.C. Strain, O. Farkas, J. Tomasi, V. Barone, M. Cossi, R. Cammi, B. Mennucci, C. Pomelli, C. Adamo, S. Clifford, J. Ochterski, G.A. Petersson, P.Y. Ayala, Q. Cui, K. Morokuma, D.K. Malick, A.D. Rabuck, K. Raghava-chari, J.B. Foresman, J. Cioslowski, J.V. Ortiz, B.B. Stefanov, G. Liu, A. Liashenko, P. Piskorz, I. Komaromi, R. Gomperts, R.L. Martin, D.J. Fox, T. Keith, M.A. Al-Laham, C.Y. Peng, A. Nanayakkara, C. Gonzalez, M. Challacombe, P.M.W. Gill, B. Johnson, W. Chen, M.W. Wong, J.L. Andres, C. Gonzalez, M. Head-Gordon, E.S. Replogle, J.A. Pople, Computer Code GAUSSIAN 98, Revision A.6, Gaussian Inc., Pittsburgh, PA, 1998.
[31] E.F. Archibong, A. St-Amant, J. Chem. Phys. 109 (1998) 962.
[32] E.F. Archibong, A. St-Amant, Chem. Phys. Lett. 284 (1998) 331.
[33] E.F. Archibong, A. St-Amant, J. Phys. Chem. A 102 (1998) 6877.
[34] E.F. Archibong, A. St-Amant, J. Phys. Chem. A 103 (1999) 1109.
[35] E.F. Archibong, A. St-Amant, Chem. Phys. Lett. 316 (2000) 151.
[36] A.D. McLean, G.S. Chandler, J. Chem. Phys. 72 (1980) 5639.
[37] M.J. Frisch, et al., GAUSSIAN 94, Gaussian, Pittsburgh, PA, 1995.
[38] Z.Y. Liu, C.R. Wang, R.B. Huang, Int. J. Mass Spectrom. Ion Processes 4 (1995) 201.
[39] E.F. Archibong, A. St-Amant, J. Phys. Chem. A 106 (2002) 7390.
[40] P. Piquini, S. Canuto, A. Fazzio, Nanostruct. Mater. 10 (1998) 635.
[41] T.R. Talor, K.R. Asmis, C. Xu, D.M. Neumark, Chem. Phys. Lett. 297 (1998) 133.